CORROSION SCIENCE AND TECHNOLOGY, Vol.23, No.4(2024), pp.255~265 pISSN 1598-6462 / eISSN 2288-6524
[Research Paper] DOI: https://doi.org/10.14773/cst.2024.23.4.255

Effect of Seawater Concentration on Electrochemical Corrosion of Duplex Stainless Steel

Ho-Seong Heo[1], Hyun-Kyu Hwang[2], Dong-Ho Shin[2], and Seong-Jong Kim[3,†]

[1]*SNNC, 2148-139, Jecheol-ro, Gwangyang-si, Jeollanam-do, 57812, Korea*
[2]*Department of marine engineering, Graduate school, Mokpo national maritime University, 91, Haeyangdaehak-ro, Mokpo-si, Jeollanam-do, Korea*
[3]*Division of marine system engineering, Mokpo national maritime university, 91, Haeyangdaehak-ro, Mokpo-si, Jeollanam-do, Korea*
(Received March 03, 2024; Revised March 03, 2024; Accepted March 12, 2024)

Duplex stainless steels (UNS S32205, UNS S32750) are used in various environments. The potentiodynamic polarization tests were conducted at 30 °C in order to study the electrochemical corrosion behaviors of duplex stainless steels under different seawater concentrations (fresh water, seawater, mixed water). The results of Tafel analysis in seawater showed that UNS S32205 and UNS S32750 had the highest corrosion current densities at 6.12×10^{-4} mA/cm^2 and 5.41×10^{-4} mA/cm^2, respectively. The pitting potentials of UNS S32205 and UNS S32750 were comparable to or higher than the oxygen evolution potential in fresh water, mixed water, and seawater. The maximum damage depths and surface damage ratio caused by pitting corrosion increased with chloride concentration. The synergy effect of molybdenum and nitrogen enhances the concentration of Mo, Ni, and Cr at the interface of the metal-electrolyte. In particular, in the case of nitrogen, NH_3 and NH_4^+ are formed to compensate for the pH drop in the pitting region, thereby strengthening the repassivation of the film. The excellent corrosion resistance of UNS S32750 is attributed to the strengthening effect of the chromium oxide film due to the presence of molybdenum and nitrogen.

Keywords: *Duplex stainless steel, UNS S32205, UNS S32750, Seawater concentration, Electrochemical corrosion*

1. Introduction

Since the concentration of chlorine ions (Cl^-) in the marine environment is higher than that of in freshwater, marine equipment and devices materials under marine environment are exposed to severe corrosive conditions [1-4]. Stainless steel forms a passive film (Cr_2O_3), has excellent corrosion resistance, and has sufficient strength, so it is a material widely used in marine environment. However, local corrosions such as pitting corrosion, crevice corrosion, and stress corrosion cracking in neutral salt solutions remain as a problem of stainless steel [5]. Stainless steels mainly used in various industrial fields are ferritic and austenitic stainless steels. Duplex stainless steel has a structure in which ferritic and austenitic phases are very finely combined with a ratio of about 50:50, and its yield strength is 2-3 times higher compared to that of austenitic stainless steel [6]. In the early stages of development of duplex stainless steel, the range of use was very limited due to reduced corrosion resistance and ductility at welding parts. However, the distribution of chromium in ferritic and austenitic phases was uniformed by adding 0.15 to 0.25% nitrogen. In addition, the resistance for stress corrosion cracking, pitting and crevice corrosion were improved in a chlorine atmosphere [7]. Recently, duplex stainless steel has been manufactured by containing 25% or more of chromium to improve mechanical strength and corrosion resistance compared to the existing duplex stainless steel having a chromium content of 22%. Investigations on duplex stainless steels are changes of phase fractions with heat treatment temperature and time, comparison of pitting resistance with temperature, and pitting caused by mixing of non-metallic inclusions. However, there are few studies on the corrosion of duplex stainless steels with chlorine ion concentration. In particular, large ships navigate not only in marine environments (Pacific, Atlantic, etc.) but also in freshwater environments (Yangtze River, Panama

[†]Corresponding author: ksj@mmu.ac.kr
Ho-Seong Heo: Assistant manager, Hyun-Kyu Hwang: Graduate Student, Dong-Ho Shin: Graduate Student, Seong-Jong Kim: Professor

Canal, etc.) and operate in various environments. Therefore, in this study, the effects of seawater concentration on the electrochemical corrosion of duplex stainless steel were investigated.

2. Experimental method

The specimens used in this research were duplex stainless steels UNS S32205 (stainless steel 329J3L) and UNS S32750 (stainless steel 329J4L) which improved corrosion resistance by increasing the amount of chromium. Potentiodynamic polarization tests were conducted to evaluate the corrosion resistance of UNS S32205 and UNS S32750 in various seawater concentrations. In order to figure out the corrosion characteristics in various chloride concentrations, seawater, freshwater and mixed water (seawater: freshwater = 1:1) were used as electrolytes to compare and analyze the electrochemical behaviors. The chemical compositions of duplex stainless steels UNS S32205 and UNS S32750 are listed in Table 1 The specimens were processed with a size of 10 mm × 10 mm using a cutting machine supplied with cooling water to minimize thermal deformation, and mounted with epoxy resin. After mounting, the specimens were polished step by step up to SiC paper #600. Thereafter, the specimens were cleaned with ultrasonic cleaning for 3 minutes in acetone and distilled water, and dried in a vacuum chamber for 24 hours. The main components and properties of the experimental solutions are shown in Table 2 Potentiodynamic polarization experiments and Tafel analyses were conducted to evaluate the corrosion resistance in various chloride concentrations, using the FR/VCP of BioLogic Science Instruments Co. In the polarization tests, a silver/silver chloride (Ag/AgCl) electrode and a platinum (Pt) electrode were used as the reference electrode and counter electrode. The electrochemical corrosion characteristics were compared with natural seawater, fresh water and mixed water at 30 ºC as electrolytes. The potentiodynamic polarization tests after immersion during 3600s were carried out from 0.25 V to 2.0 V (vs. open circuit potential) with scanning rate of 1.67 mV/s. The pitting potential (E_{pit}) was calculated through the potentiodynamic polarization curve. In addition, the corrosion current density (I_{corr}) and the corrosion potential (E_{corr}) were calculated using the Tafel extrapolation method. After the experiments, the surfaces were analyzed using a scanning electron microscope (SEM, BRUKER, SNE-4500M Plus) and a 3D optical microscope (Motic, PSM-100, I-solution) to figure out the corrosion tendency. Etching was carried out in 40% NaOH aqueous solution under DC 6 V, 5s conditions to observe the phase fractions, microstructures of the ferritic and the austenitic phases. Thereafter, the phase fractions were analyzed through image analysis.

3. Results and discussion

Fig. 1 presented analysis results of the phase fractions and micro structures. When duplex stainless steels UNS S32205 and UNS S32750 were etched, an α-ferritic (dark side) phase and a γ-austenitic (bright side) phase

Table 1. Chemical compositions of UNS S32205 and UNS S32750 (wt%)

	C	Si	Mn	S	Cr	Ni	Mo	Cu	N	Fe
UNS S32205	0.026	0.48	1.64	0.001	22.4	5.69	3.03	0.19	0.17	Bal
UNS S32750	0.023	0.48	0.75	0.001	25.3	7.33	3.14	0.155	0.191	Bal

Table 2. Chemical compositions and properties of electrolyte (wt%)

	Main component (mg/L)						pH	Dissolved oxygen (mg/L)	Electric conductivity (mS/cm)
	SO_4^{2-}	Cl^-	Na^+	K^+	Mg^{2+}	Ca^{2+}			
Sea water	1746	15721	8401	344	1121	357	7.90	16.1	45.3
Mixed water	1073	9989	5367	218	695	237	7.75	16.0	29.10
Fresh water	333	3267	368	77	225	104	7.52	16.0	11.16

	UNS S32205	UNS S32750
Surface image	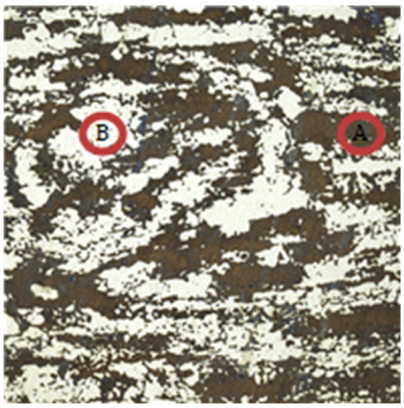	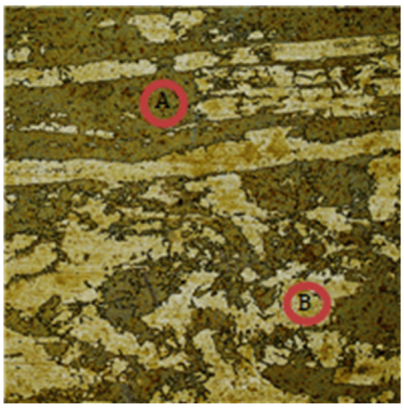
Image analysis	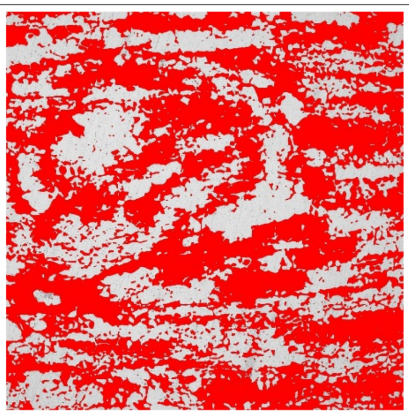	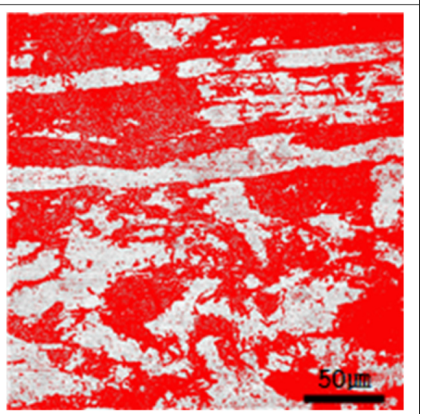
Phase fraction	A = α Ferrite (44%) B = γ Austenite (56%)	A = α Ferrite (45%) B = γ Austenite(55%)

Fig. 1. Metallographic analysis and phase fraction of UNS S32205 and UNS S32750

were observed. Through the results of image analysis, it could be identified that the ratio of ferrite to austenite was about 44:56 in UNS S32205, and 45:55 in UNS S32750, which were almost the same. Experimental results related to the pitting corrosion of duplex stainless steels in chloride solutions are diverse. In particular, the results of investigation on pitting corrosion and repassivation for duplex stainless steel (UNS S31803 and UNS S32750) with temperatures, the ferritic phase had a higher pitting resistance equivalent number (PREN) than the austenitic phase, and pitting corrosion occurred preferentially in the austenitic phase rather than the ferritic phase [8]. However, study on the correlation between the phase fraction and pitting corrosion of UNS S32101, the PREN of the ferritic phase was lower than that of the austenitic phase. And, as the phase fraction of ferritic increases by heat treatment, the pitting potential moved toward negative potential so that pitting corrosion occurred preferentially in the ferritic phase. In addition, as the ferritic phase increased by heat treatment, the corrosion rate increased due to the increase of current density by the galvanic couple [9]. Therefore, the phase fraction becomes an important element in corrosion resistance. The PREN is a value indicating the resistance to pitting corrosion of stainless steel in chloride-containing environments, and it is determined by the contents of chemical elements. Elements affecting the PREN are mainly Cr, Mo, W and N. The contribution degree of these elements to PREN is as shown in the equation below.

Table 3. The chemical composition (wt%) and PREN of the two phases in UNS S32205 and UNS S32750

Materials	Phase	Cr	Ni	Mo	N	PREN
UNS S32205	Austenite	20.61	8.46	1.92	0.38	33.03
	Ferrite	24.52	5.31	3.21	0.05	35.91
	Both phases	22.40	5.69	3.03	0.17	35.17
UNS S32750	Austenite	23.21	9.86	2.42	0.40	37.60
	Ferrite	27.47	6.22	3.72	0.05	40.50
	Both phases	25.30	8.04	3.07	0.19	38.47

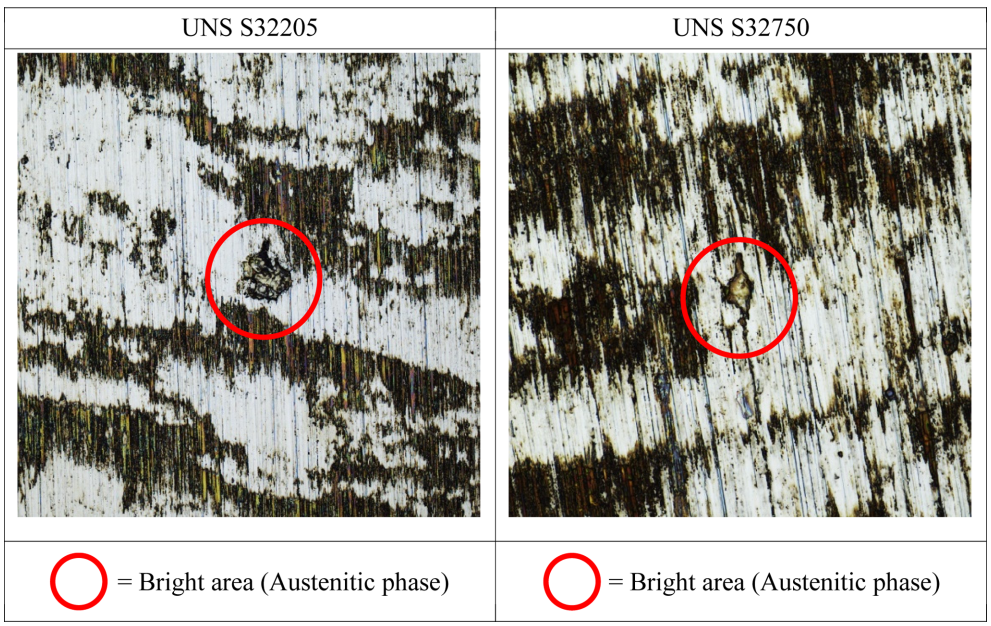

Fig. 2. Selective corrosion of UNS S32205 and UNS S32750 after potentiodynamic polarization in fresh water

$$PREN = \%Cr + 3.3\%(Mo + 0.5\%W) + 16\%N \quad (1)$$

According to this formula, stainless steels with a PREN index of 40 or more are called super stainless steel. Super stainless steels have excellent corrosion resistance in harsh environments such as marine environments and petrochemical industries. Table 3 is the result of EDS analysis and PREN values for ferritic and austenitic phases of UNS S32205 and UNS S32750. In both specimens, the contents of Cr and Mo (ferrite stabilizing elements) in the ferritic phase were higher. And the contents of Ni and N (austenite stabilizing elements) in the austenitic phase were higher. The PREN values of ferritic phase for UNS S32205 and UNS S32750 are 35.91 and 40.50, and those of austenitic phase are 33.03 and 37.60, respectively.

Fig. 2 presented surface morphologies of UNS S32205 and UNS S32750 after potentiodynamic polarization experiment in freshwater. The pitting corrosion at all specimens occurred selectively in the austenitic phase. This is consistent with the results of studies in which the austenitic phase of 2205 duplex stainless steel was selectively corroded in 0.01 mol/L NaCl solution [10]. According to various investigations on pitting corrosion of duplex stainless steel, the selective corrosion of ferritic and austenitic phases is affected by the contents of Cr, Mo, N and solution parameters. In the case of stainless steel with high contents of Cr and Mo (ferrite stabilizing elements) and a low N content, selective corrosion occurred at the austenitic phase in a neutral chloride solution. However, selective corrosion at the ferritic phase occurred when the content of Ni and N (austenite stabilizing elements) was high and Cr and Mo content was low.

Fig. 3 and Fig. 4 displayed the results of potentiodynamic polarization experiments for duplex stainless steels UNS S32205 and UNS S32750 in fresh water, seawater and mixed water at 30 ºC. The passivation was observed where the increase of current density was stagnant due to the passive film (Cr_2O_3) formed at the initial stage of immersion. The pitting potentials of UNS S32205 and UNS were not clearly determined by oxygen evolution in fresh water, mixed water, and seawater. The oxygen evolution ($4OH^- \rightarrow O_2 + 2H_2O + 4e$) reaction in a neutral solution at pH 7 is about 1000 mV when Ag/AgCl (saturated KCl) reference electrode is used. As a result of potentiodynamic polarization, the exact value of the pitting potential cannot be confirmed due to the increase of current density by oxygen evolution, but it can be confirmed that it has a similar or higher value than the oxygen evolution potential. As a result of the potentiodynamic polarization of duplex stainless steel in a neutral chloride solution, there are many researches that did not measure exact pitting potential due to oxygen evolution [11,12]. It means UNS S32205 and UNS S32750 have a higher pitting resistance compared to UNS S30400 and UNS S31603 which are common austenitic stainless steel widely used commercially. Since pitting corrosion begins at E_{pit} (pitting potential), the value of E_{pit} represents a measure on the pitting corrosion resistance. It can be seen that the pitting corrosion resistance of UNS S32205 and UNS S32750 are nobler than commonly used austenitic stainless steels because the contents of Cr, Mo, and N that affecting the PREN are higher.

Fig. 5 presented a schematic diagram of the passive film applied with bipolar model. MoO_4^{2-} acts as an electron acceptor on the surface of passivation film due

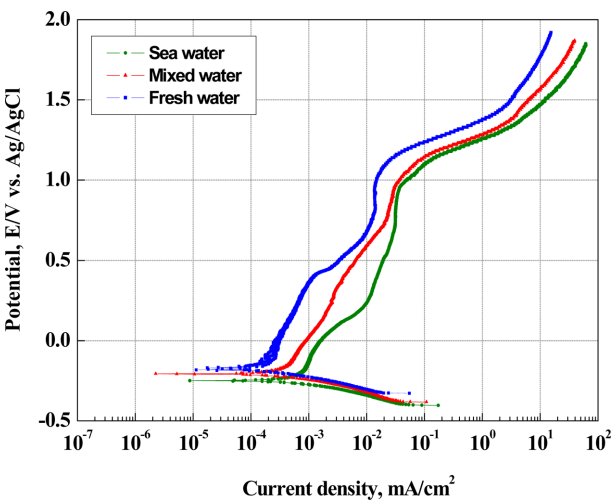

Fig. 3. Potentiodynamic polarization curves of UNS S32205 in various solutions

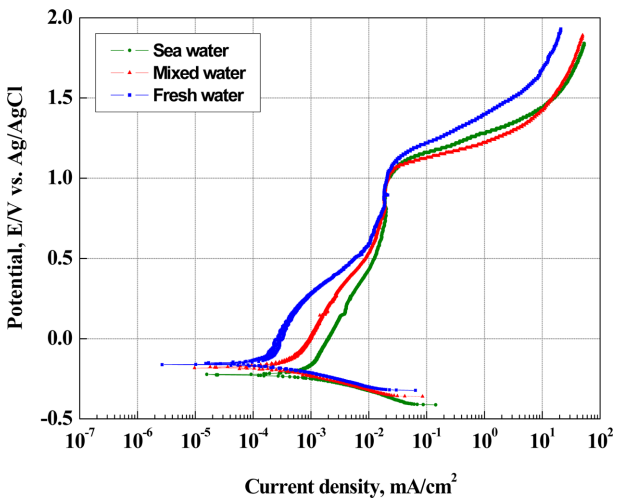

Fig. 4. Potentiodynamic polarization curves of UNS S32750 in various solutions

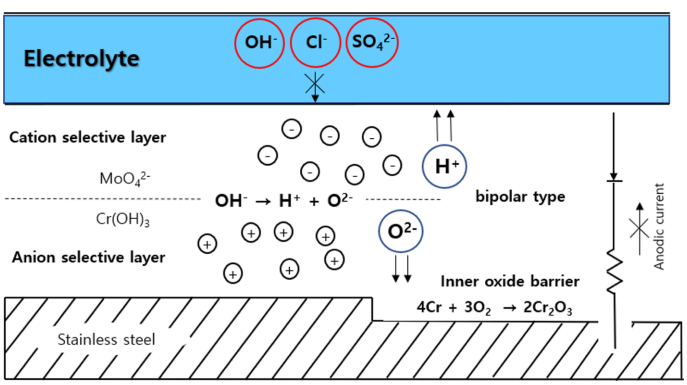

Fig. 5. Schematic diagram of enhanced passive film formation by Molybdenum [13](Positive charge : + , Negative charge : -)

to addition of Mo. Thus, the strengthening of metal and oxygen combination reinforces lattice structure of the passive film [13]. With bipolar model of passive films, the absorption of MoO_4^{2-} in the film due to addition of Mo forms a cation selective layer, and promotes dehydrogenation of the film [14]. The passive film is strengthened with production of chromium oxide film (Cr_2O_3) as the O^{2-} formed by dehydrogenation is transferred to the metal surface. The passive film is strengthened by this mechanism. In addition, the cation selective layer in the outer layer of film inhibits the ingression of OH^- and Cl^- so that the rehydration can be efficiently stopped [13,15]. The dehydrogenation reaction starts when chromium hydroxide ($Cr(OH)_3$) is decomposed into chromium oxide (Cr_2O_3), hydroxyl ions (OH^-) and hydrogen ions (H^+). The formed OH^- are decomposed into O^{2-} and H^+. The H^+ move through the cation selective layer and outside of film. The O^{2-} are combined with Cr to form chromium oxide films (Cr_2O_3), and corrosion resistance is improved [16]. The entire dehydrogenation reaction is as follows.

$$Cr + Cr(OH)_3 \rightarrow Cr_2O_3 + 3H \quad (2)$$

Fig. 6 displayed results of analysis of polarization curves and Tafel analysis after the potentiodynamic polarization experiments for UNS S32205 and UNS S32750. It is considered that Cl^- ions were replaced by oxygen or hydroxyl groups in the part where passive film is somewhat unstable. This results lead to the local dissolution of the film [17]. In seawater, it has the highest electrical conductivity, the corrosion potentials (E_{corr}) of UNS S32205 and UNS S32750 showed the most negative potentials of -0.248 V and -0.223 V, and the corrosion current density (I_{corr}) presented the highest values of 6.12×10^{-4} mA/cm^2 and 5.41×10^{-4} mA/cm^2, respectively. This is considered to be because the influence of Cl^- ions on the corrosion characteristic in seawater is greater than in freshwater. The corrosion potential shifted to the negative direction potentials and the corrosion current density increased with chloride concentration raise. However, pitting potential showed to be comparable to or higher than the oxygen evolution potential despite the increase of chloride concentration. The reason is considered to be the synergy effect of Mo and N. Synergy effect of Mo and N enhances the concentration of Mo, Ni and Cr at the metal-electrolyte interface of initiated pitting. The N reacts with H^+ to form NH_3 and NH_4^+ and is expected to compensate for pH drop of pitting region. The repassivation of the film by this mechanism is enhanced by increased pH. In

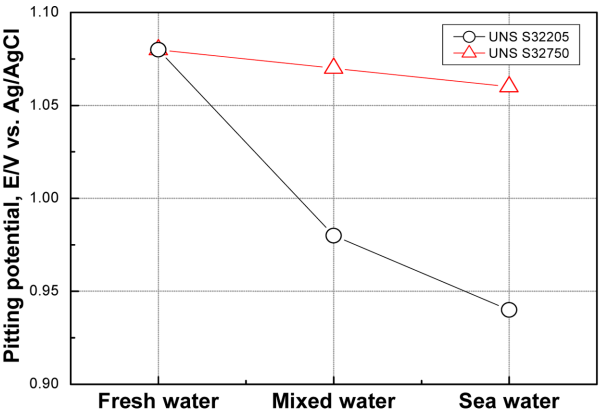

(a) Pitting potential

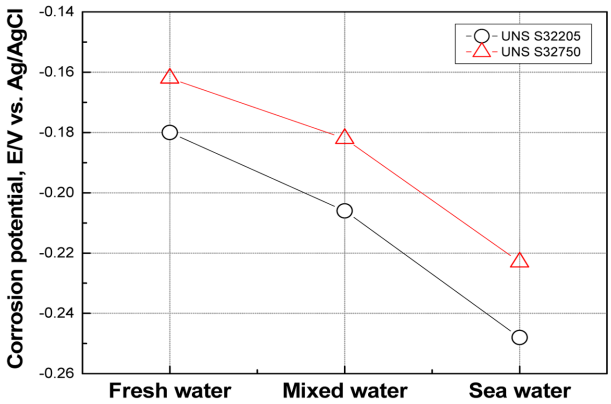

(b) Corrosion potential

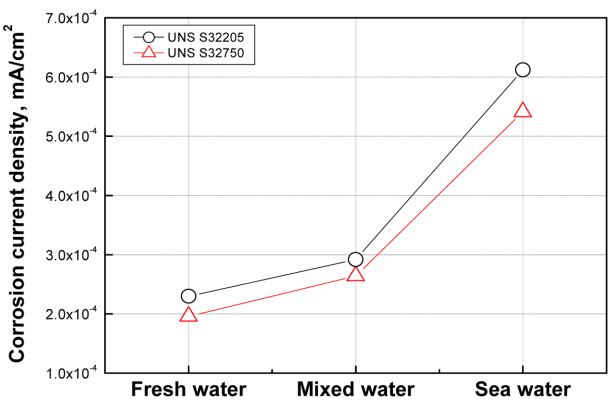

(c) Corrosion current density

Fig. 6. Results of polarization curves analysis and Tafel analysis after potentiodynamic experiments for each specimen in various solutions

addition, NO_x^- species enhances the cation selectivity of passive film. Therefore, the oxide content and the density of the film is increased. The NO_x^- acts similarly to a potent inhibitor in passive film at active site to promotes the formation of chromium oxide. Consequently, NO_x^- reacts with Mo to produce more molybdate and nitric oxide, which helps improve corrosion resistance [18].

Fig. 7 displayed the analysis results of surface morphologies and maximum damage depths using a 3D microscope after potentiodynamic polarization experiment. The pitting corrosion damages in UNS S32205 and UNS

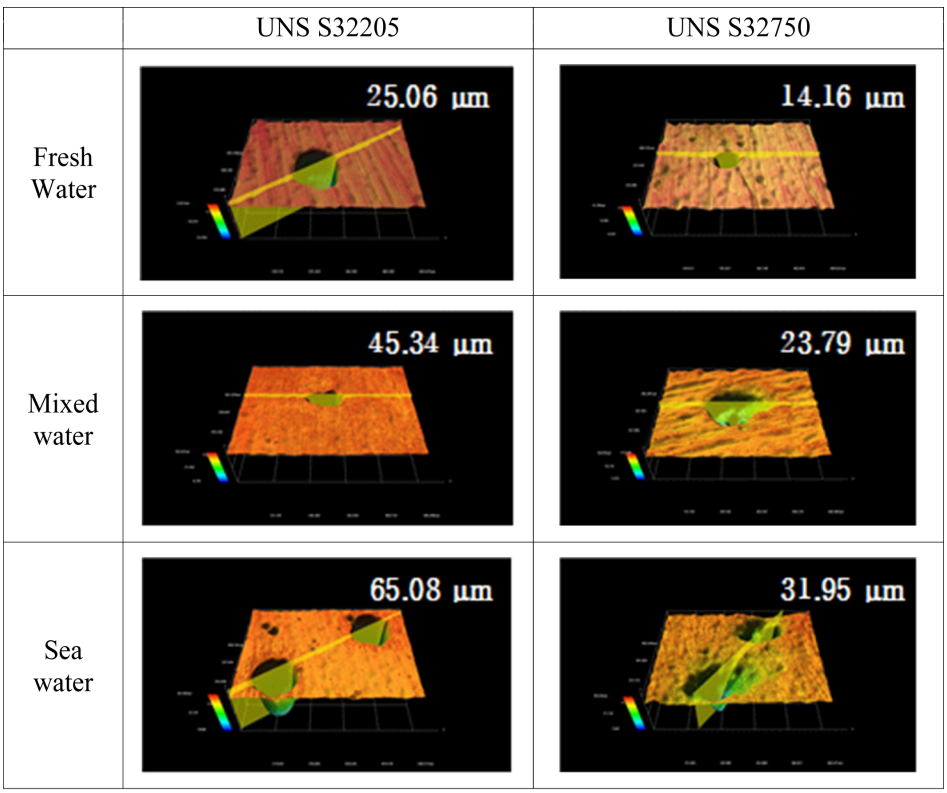

(a) 3D analysis

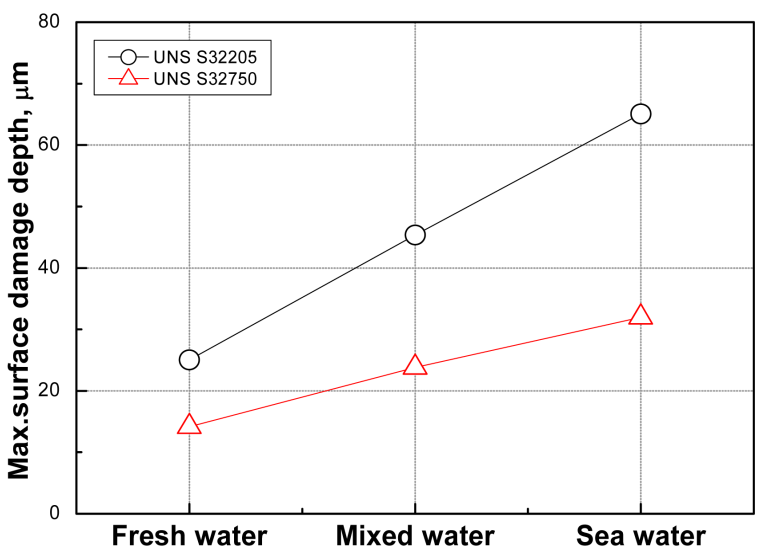

(b) Max. surface damage depth

Fig. 7. 3D analysis results of UNS S32205 and UNS S32750 after potentiodynamic polarization experiment in various solutions

		Fresh water	Mixed water	Sea water
UNS S32205	Damaged area		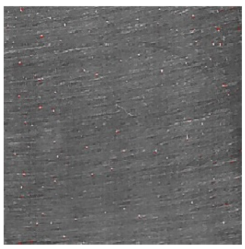	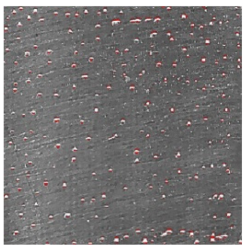
	ratio	0.00%	0.13%	0.97%
UNS S32750	Damaged area		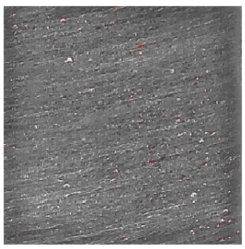	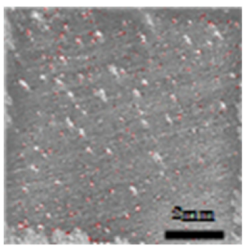
	ratio	0.00%	0.20%	0.99%

Fig. 8. Appearance of UNS S32205 and UNS S32750 after potentiodynamic polarization experiment in various solutions

S32750 were observed in all solutions, and pitting corrosions were formed wider and deeper in mixed water and seawater than in freshwater. The maximum pitting depths of UNS S32205 in mixed water and seawater were 45.340 μm and 65.080 μm, which were 1.80 and 2.59 times higher than that of fresh water. The maximum pitting depths of UNS S32750 in mixed water and seawater were 23.790 and 31.951, which were 1.68 and 2.26 times higher than those of fresh water. The distribution and size of pitting corrosion increased with chloride concentration. This is consistent with the result of the investigation that the higher chloride concentrations accelerates the internal electron transfer of Cl^- which is favorable for micropits to maintain growth and can lead to faster growth [19].

Fig. 8 displayed the surface scan and pitting corrosion damage ratio after potentiodynamic polarization experiment. The pitting corrosion damage of UNS S32205 and UNS S32750 could be hardly identified in fresh water but could be found in mixed water and seawater. The UNS S32750 which has excellent pitting resistance, presented high damage ratio by pitting corrosion than UNS S32205. This result is also consistent with the surface morphologies observed with SEM after the potentiodynamic polarization test in Fig. 9. The pitting corrosion damage in fresh water, which was not observed at the result of surface scan, was found, and it could be seen that the size and number of pits increased with chloride concentration. At the analysis results of 3D micrography and pitting corrosion damage ratio, the pitting corrosion grows to depth direction in UNS S32205 while the distribution of pitting corrosion increased in UNS S32750. The sizes and depths of pitting corrosion in UNS S32750 are smaller than those in UNS S32205. In addition, the distribution of pitting corrosion in UNS S32750 is larger than that of UNS S32205. It is presumed to be the difference in current density after oxygen evolution potential.

Fig. 10 compared the current density values a t +1.5 V (vs. Ag/AgCl) after oxygen evolution. The difference of the current density values in fresh water is little. The current density values of UNS S32750 in mixed water and seawater presented 14.59 mA/cm^2 and 16.10 mA/cm^2, respectively, which are 2.29 and 1.34 times higher than those of UNS S32205. Despite the high current density, pitting resistance of UNS 32750 is

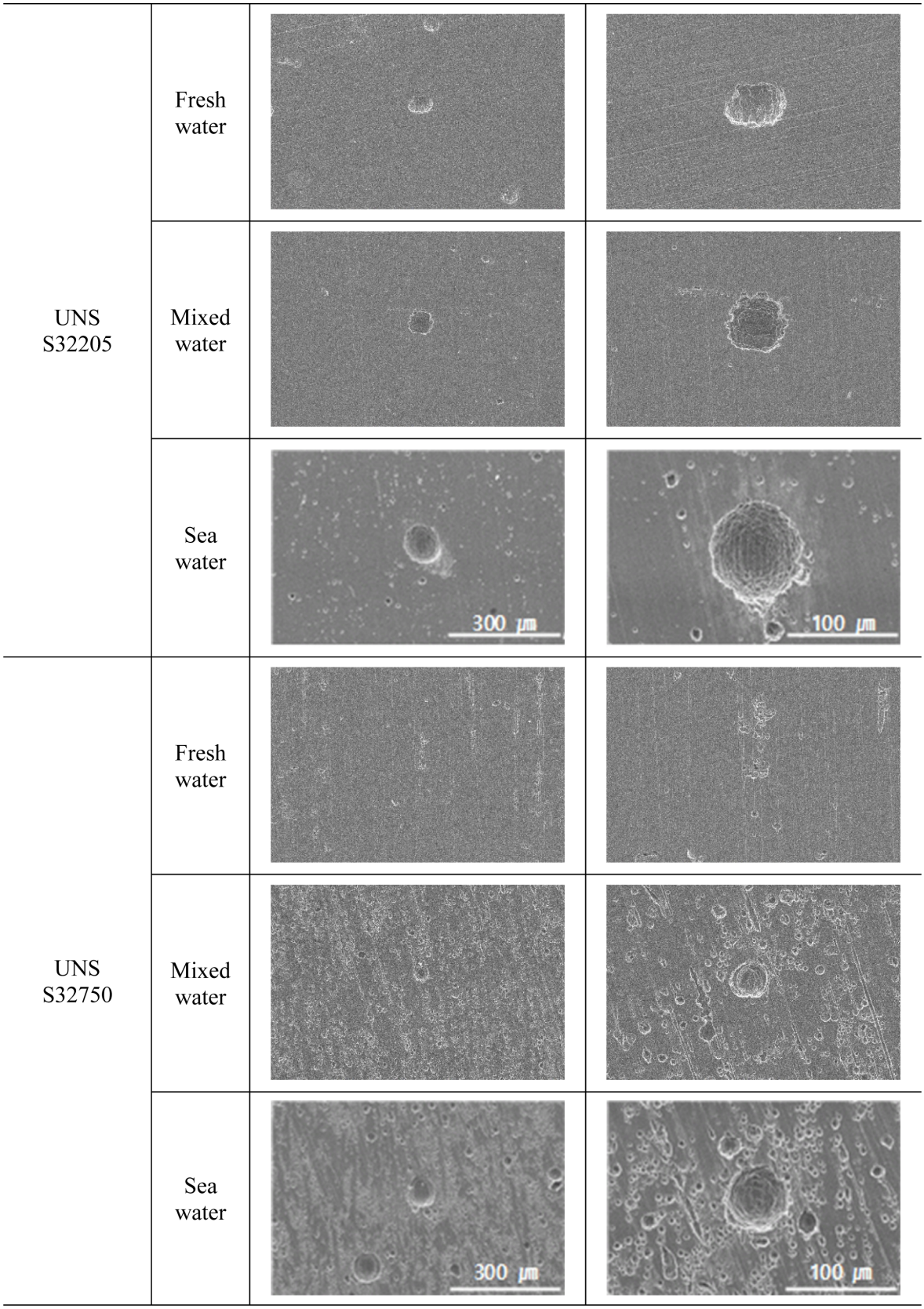

Fig. 9. Surface morphologies after potentiodynamic polarization experiment of UNS S32205 and UNS S32750 in various solutions

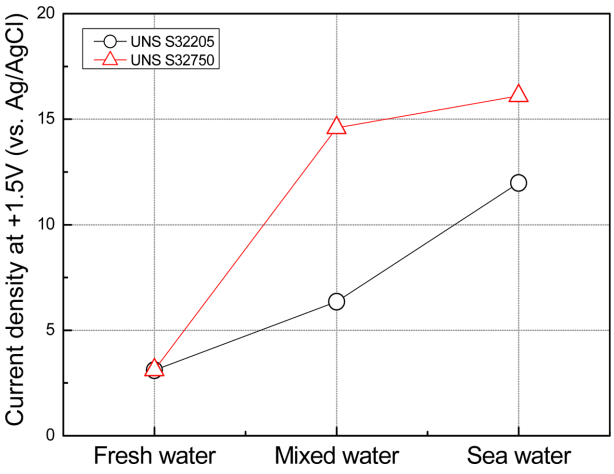

Fig. 10. Current density at +1.5 V (vs. Ag/AgCl) of UNS S32205 and UNS S32750 in various solutions

excellent because pits do not grow to the depth direction but are widely distributed on the surface.

4. Conclusion

Through the electrochemical experiments of duplex stainless steels UNS S32205 and UNS S32750 with seawater concentration, following conclusions were obtained.

1. The phase fractions of the ferritic phase and the austenitic phase were α:γ=44:56 in UNS S32205 and α:γ=45:55 in UNS S32750, respectively. Therefore, no significant difference was shown in phase fractions.

2. At the result of potentiodynamic polarization experiments, UNS S32205 and UNS S32750 showed the pitting potential were comparable to or higher than oxygen evolution potential in fresh water, mixed water and seawater.

3. At the result of Tafel analysis, seawater presented the highest corrosion current density followed by mixed water and fresh water in order. And the lowest corrosion current density (1.96×10^{-4} mA/cm^2) was presented at the freshwater condition of UNS S32750, indicating excellent corrosion resistance.

4. The maximum damage depth of UNS S32205 increased from 25.06 to 65.08 with chloride concentration increment. Pit grew to the depth direction and the distribution presented a smaller tendency than UNS S32750.

5. The maximum damage depths of UNS S32750 are smaller than those of UNS S32205, but the distribution of the pitting is larger. Corrosion resistance of UNS S32750 is excellent in various environment from the perspective of depth growth of pit.

References

1. H. K. Hwang, S. J Kim, Effect of Seawater Temperature on the Cyclic Potentiodynamic Polarization Characteristics and Microscopic Analysis on Damage Behavior of Super Austenitic Stainless Steel, *Corrosion science and technology*, **20**, 412 (2021). Doi: https://doi.org/10.14773/cst.2021.20.6.412
2. H. K. Hwang, S. J Kim, Investigation of the Electrochemical Characteristics of Electropolished Super Austenite Stainless Steel with Seawater Temperature, *Corrosion science and technology*, **22**, 164 (2023). Doi: https://doi.org/10.14773/cst.2023.22.3.164
3. M. H. Im, Cavitation Characteristics on Impeller Materials of Centrifugal Pump for Ship in Sea Water and Fresh Water, *Corrosion science and technology*, **10**, 218 (2011). https://www.j-cst.org/opensource/pdfjs/web/pdf_viewer.htm?code=C00100600218
4. H. Ezuber, A. El-Houd, and F. El-Shawesh, A study on the corrosion behavior of aluminum alloys in seawater, *Materials & Design*, **29**, 801 (2008). Doi: https://doi.org/10.1016/j.matdes.2007.01.021
5. R. Devaux, D. Vouagner, A. M. De Becdelievre and C. Duret-thual, Electrochemical and surfaces studies of the ageing of passive layers grown on stainless steel in neutral chloride solution, *Corrosion Science*, **36**, 171 (1994). Doi: https://doi.org/10.1016/0010-938X(94)90118-X
6. J. R. Davis ed., ASM Specialty Handbook Stainless Steels, p. 13, ASM International, OH (1994).
7. J. D. Redmond, Materials Engineering, **27**, 153 (1986).
8. Bo Deng, Yiming Jiang, Jia Gong, Cheng Zhong, Juan Gao, Jin Li, Critical pitting and repassivation temperatures for duplex stainless steel in chloride solutions, *Electrochimica Acta*, **53**, 5220 (2008). Doi: https://doi.org/10.1016/j.electacta.2008.02.047
9. Heon-Young Ha, Tae-Ho Lee, Chang-Geun Lee, Hanme Yoon, Understanding the relation between pitting corrosion resistance and phase fraction of S32101 duplex stainless steel, *Corrosion Science*, **149**, 226 (2019). Doi: https://doi.org/10.1016/j.corsci.2019.01.001
10. TSAI Wen-Ta1, TSAI Kuen- Ming, L IN Chang-jian, FU

Yan, Selective corrosion in duplex stainless steel, *Journal of Electrochemistry*, **9**, 170 (2003). Doi: https://doi.org/10.61558/2993-074X.1501

11. R. Sriram and D. Tromans, Pitting Corrosion of Duplex Stainless Steels, *Corrosion*, **45**, 804 (1989). Doi: https://doi.org/10.5006/1.3584986
12. R. Magnabosco and N. A. Falleiros, Pit Morphology and its Relation to Microstructure of 850°C Aged Duplex Stainless Steel, *Corrosion*, **61**, 130 (2005). Doi: https://doi.org/10.5006/1.3278167
13. A. R. Brooks, C. R. Clayton, K. Doss, and Y. C. L, On the Role of Cr in the Passivity of Stainless Steel, *Journal of The Electrochemical Society*, **133**, 2459 (1986). Doi: https://doi.org/10.1149/1.2108450
14. M. Sakashita and N. Sato, The effect of molybdate anion on the ion-selectivity of hydrous ferric oxide films in chloride solutions, *Corrosion Science*, **17**, 473 (1977). Doi: https://doi.org/10.1016/0010-938X(77)90003-8
15. C. R. Clayton and Y. C. Lu, A Bipolar model of the Passivity of Stainless steel, *Journal of The Electrochemical Society*, **133**, 2465 (1986). Doi: https://doi.org/10.1149/1.2108451
16. Y. S. Cho, Effects of Mo Content and Ion-Nitriding on the Pitting Behavior of STS 304 Stainless Steel, pp. 6 – 7, Graduate School Chonnam National University (1994).
17. K. W. Nam, J. E. Paeng and K. Y. Kim, Immersion Characteristics of STS316L with Degree of Different Cold Rolling, *Journal of Power System Engineering*, **24**, 90 (2020). Doi: https://doi.org/10.9726/KSPSE.2020.24.3.090
18. Y. S. Kim, Synergistic Effect of Nitrogen and Molybdenum on Localized Corrosion of Stainless Steels, *Corrosion Science and Technology*, **9**, 20 (2010). https://www.j-cst.org/opensource/pdfjs/web/pdf_viewer.htm?code=C00090100020
19. Yu Zuo, Haitao Wang, Jingmao Zhao, Jinping Xiong, The effects of some anions on metastable pitting of 316L stainless steel, *Corrosion Science*, **22**, 13 (2002). Doi: https://doi.org/10.1016/S0010-938X(01)00031-2